
Monograph:
Knox, C orcid.org/0000-0002-4673-5649, Rogers, M orcid.org/0000-0002-4550-2392 and Moorsom, T (2020) Van der Waals epitaxy of C_{60} on the topological insulator Bi_2Se_3. Report. Materials from the Royce Deposition System (2). University of Leeds

https://doi.org/10.48785/100/81

Van der Waals epitaxy of C_{60} on the topological insulator Bi_2Se_3

C.S.Knox, M.D.Rogers, T.Moorsom

This application note describes the growth of a novel Bi_2Se_3/ C_{60} heterostructure in the Royce deposition system at the University of Leeds. We also present structural characterisation and transmission electron microscopy data in order to understand nature of the Bi_2Se_3/ C_{60} interface.

1 Introduction

Bismuth selenide (Bi_2Se_3) has attracted much experimental interest as an archetypal 3D topological insulator, where transport is dominated not by the insulating bulk band alignment, but by metallic, spin-polarised surface states [1]. As long as time-inversion symmetry remains unbroken, these surface states are protected against elastic back-scattering, as such an event would require a spin-flip [2]. Bi_2Se_3 grows with a layered crystal structure, where atomic layers in the sequence Se-Bi-Se-Bi-Se (so-called quintuple layers) are separated by a van der Waals (vdW) gap between the selenium atoms [3]. This allows Bi_2Se_3 to be grown on a wide variety of substrates [1, 4, 5], as the growth is initiated by a vdW gap between the substrate and the Bi_2Se_3, without the need for a strained interfacial layer, in a process known as van der Waals epitaxy [6]. Additionally, as a Bi_2Se_3 quintuple layer is terminated by a passivated selenium layer, a vdW gap can form between the Bi_2Se_3 and a subsequently deposited material [7]. It has recently been noted that buckminsterfullerene (C_{60}) also orders surprisingly well on a Bi_2Se_3 substrate [8].

Previously, it has been noted that the electronic structure of a C_{60} molecular film is highly substrate dependant, due to charge-transfer induced band broadening [9–11]. However, recent observations of bulk-like C_{60} bands on a Bi_2Se_3 substrate seem to indicate that there is very little hybridisation between the Bi_2Se_3 bulk and the C_{60} [8, 12]. As the molecular orbitals within the C_{60} can be tuned by an applied gate bias [13], this presents an interesting opportunity investigate the hybridisation between the topological surface states and the bands of C_{60} [14, 15].

Here we report on the novel growth of a bilayer Bi_2Se_3/C_{60} heterostructure grown in the Royce thin film deposition system at the University of Leeds. The bulk crystal structure of the Bi_2Se_3 and the C_{60} is probed by Raman spectroscopy and X-ray diffraction measurements, which show that both materials within this heterostructure are well ordered in a strain-free, bulk-like manner. We also examine the Bi_2Se_3/C_{60} interface under transmission electron microscopy (TEM) at the LEMAS facility at the University of Leeds, and determine that while the C_{60} is grown by vdW epitaxy on top of completed Bi_2Se_3 quintuple layers, the existence of bismuth dangling bonds at the edge of a Bi_2Se_3 terrace disrupts the vdW epitaxy of the C_{60}, leading to the formation of a disordered region at the interface.

2 Growth

In preparation for the growth procedure, 8×8 mm [0001] oriented Al_2O_3 substrates were cleaned under ultrasonic agitation in acetone and isopropyl alcohol, in order to remove any possible organic contaminants from the dicing process. The sapphire substrate is then air-dried before being immediately loaded into the Royce thin film deposition system. Once loaded, the substrate was transferred to the Royce MBE system, where it was heated to 500 ℃ (measured by a thermocouple attached to the sample manipulator) in order to outgas the sample holder and remove any remaining contaminants from the substrate.

The Bi_2Se_3 layer was grown by evaporating bismuth and selenium from standard dual-filament Knudsen cells. The Bi:Se flux ratio, measured by an ion-gauge flux monitor, was maintained at 1:15 throughout the growth, in order to obtain stoichiometric Bi_2Se_3 and to minimise the formation of selenium vacancies [5]. In order to improve the quality of the as-grown Bi_2Se_3, a two-step process was adopted [1], whereby a thin nucleation layer of Bi_2Se_3 was grown at a lower temperature. For this study, an intentionally low temperature of at 130 ℃ was chosen, in order to study the effects of surface roughness on the ordering of the C_{60} molecular film [5]. After this nucleation layer was grown the rest of the epitaxial Bi_2Se_3 was grown at a temperature of 330 ℃.

The Bi_2Se_3 sample was then transferred through

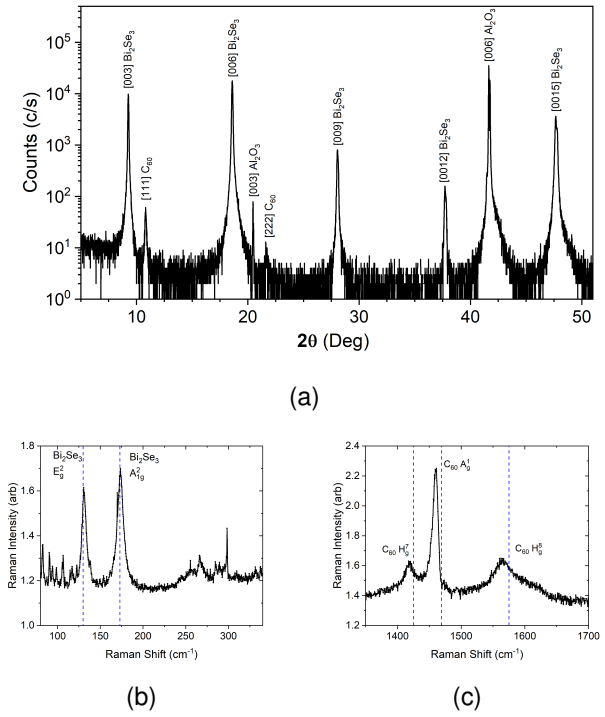

Figure 1: Structural characterisation of the Bi_2Se_3/ C_{60} sample. Panel a) depicts the X-ray diffraction spectrum of the Bi_2Se_3/ C_{60} sample, where the positions of the known diffraction peaks are labelled with the relevant material and lattice planes. Panels b) and c) show the Raman spectra of the Bi_2Se_3/ C_{60} sample, where the blue dashed lines represent the expected positions of the Raman modes. Panel b) shows the low frequency range, dominated by the Bi_2Se_3 modes, as excited by a 633 nm laser. Panel c) shows the high frequency range, dominated by the C_{60} modes, as excited by a 473 nm laser.

the radial transfer chamber under a pressure of $\approx 10^{-11}$ mbar, to the Royce organics chamber. From there, a thick C_{60} layer was grown, over the course of 20 minutes, from a standard Knudsen cell with the Bi_2Se_3 substrate at ambient temperature [16]. This structure was then capped by a 15 nm thick platinum layer, deposited via electron-beam evaporation. The thickness and deposition rate of the platinum film was monitored by a quartz crystal balance.

3 Material Properties

The X-ray diffraction (XRD) spectrum for the Bi_2Se_3/C_{60} heterostructure is shown in Fig. 1a. The sample shows clear Bi_2Se_3 peaks ordered in the $[001]$ direction, with a c-axis lattice parameter of 2.861 ± 0.007 nm, which is in agreement with the bulk lattice parameter of 2.866 nm [17]. Additionally, we can see that the inter-molecular spacing of the face centred cubic C_{60} lattice is 1.415 ± 0.007 nm, which correlates closely with the lattice spacing for bulk C_{60}, 1.42 nm [18]. This indicates that not only has the Bi_2Se_3 grown epitaxially on top of the Al_2O_3 substrate, but that the C_{60} has grown in a well ordered and relaxed manner on top of the Bi_2Se_3.

To confirm this observation, the vibrational spectrum of the Bi_2Se_3/C_{60} heterostructure was characterised by Raman spectroscopy. Two spectral ranges were considered, one between 80 and 340 cm^{-1}, which encompasses the principle phonon modes of Bi_2Se_3 (shown in Fig. 1b)[19], and the other between 1200 and 1700 cm^{-1}, detailing the vibrational spectrum of the C_{60} [20] (shown in Fig. 1c). Fig. 1b corroborates the observations from the XRD data, as the sample shows well defined Bi_2Se_3 Raman modes at 131 ± 1 cm^{-1} and 173 ± 1 cm^{-1}, indicating well relaxed Bi_2Se_3[19]. The high frequency regime also shows that we have well ordered C_{60}, with C_{60} Raman modes at 1419 ± 1 cm^{-1}, 1460 ± 1 cm^{-1} and 1566 ± 1 cm^{-1}, which correlate well with the expected positions of the C_{60} H_g^7, A_g^2 and H_g^8 Raman modes, respectively [21].

In order to discern why the C_{60} would order so well on top of the Bi_2Se_3 film, the Bi_2Se_3/C_{60} interface was examined under transmission electron microscopy (TEM) at the LEMAS facility at the University of Leeds. A scanning electron microscope image of the region examined under TEM is shown in Fig. 2a. The clear, terraced, triangular domains of the underlying Bi_2Se_3 surface are clearly visible through the C_{60} film. We note that, between these triangular domains, there are ≈ 500 nm wide voids in the Bi_2Se_3 film, formed as a result of the excessively low temperature chosen for the nucleation layer of Bi_2Se_3[5], where the C_{60} has deposited directly on the Al_2O_3 substrate. Examining the entire stack structure under TEM shows that the Bi_2Se_3 is approximately 124 ± 1 nm thick, resulting in an average growth rate of 0.295 ± 0.003 Ås^{-1} over the course of the 70 minute deposition procedure. Similarly, the C_{60} is found to be 104 ± 1 nm thick, resulting in an average growth rate of 0.833 ± 0.008 Ås^{-1}.

When the Bi_2Se_3/C_{60} interface is examined under TEM (as shown in Fig. 2b), we find that not only are the lattice planes of the Bi_2Se_3 and the C_{60} clearly vis-

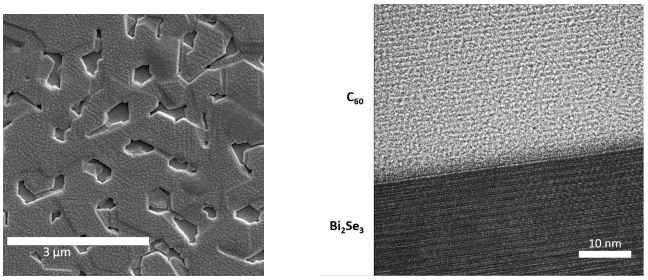

(a) (b)

Figure 2: Electron microscopy images of the Bi_2Se_3/C_{60} sample. Panel a) shows a scanning electron microscope image of the sample surface, highlighting the C_{60} grains, as well as the large triangular terraces, characteristic of Bi_2Se_3 growth. Panel b) shows a TEM image of the Bi_2Se_3/C_{60} interface, highlighting the ordered nature of both materials, and the sharp interface between them.

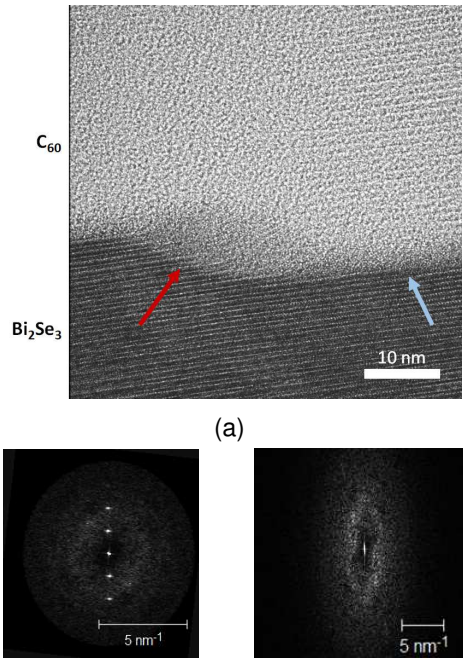

(a)

(b) (c)

Figure 3: Electron microscopy images of the Bi_2Se_3/C_{60} sample at the terrace edge of a Bi_2Se_3 domain. Panel a) shows a TEM image of the Bi_2Se_3/C_{60} interface around a terrace step. Two regions are highlighted, one where the C_{60} has grown on top of a complete Bi_2Se_3 layer (blue arrow) and another where the C_{60} has grown on top of a terrace step (red arrow). Panels b) and c) show 2D Fourier transforms of the C_{60} within the regions highlighted by the blue and red arrows, respectively.

ible, but the Bi_2Se_3/C_{60} interface is sharp, and the C_{60} is well ordered within the first few monolayers, without a strained and disordered interfacial layer. However, if we observe the Bi_2Se_3/C_{60} interface at a terrace edge on top of the triangular Bi_2Se_3 domains, as shown in Fig. 3a, we note that this is no longer the case. In fact, we find that if we take a 2D Fourier transform of the C_{60} where the molecular film is deposited on top of a terrace flat (shown in Fig. 3b), there is a clear 0.79 ± 0.02 nm periodicity, corresponding to the diameter of the C_{60} molecular cage [22]. However, if a similar Fourier transform is attempted at the step-edge of a terrace we find that the clear vertical periodicity is replaced by an amorphous ring with a similar 0.79 ± 0.02 nm periodicity, as shown in Fig. 3c.

The presence of this disordered layer at the Bi_2Se_3/C_{60} interface appears to indicate that some strain is being applied to the C_{60} by the Bi_2Se_3. This would point to the existence of dangling bonds at the step-edge of the Bi_2Se_3 terrace, which can disrupt vdW epitaxy [4, 23]. At the terrace step-edge there are exposed bismuth atoms, effectively creating a selenium vacancy at the step edge. Previously, it has been noted that selenium vacancies act as n-type donors within Bi_2Se_3[24, 25]. By freeing additional electrons, these selenium vacancies will result in the formation of dangling bismuth bonds [3]. These dangling bonds are chemically active, and so will bond to the C_{60} molecules, but as the bond angles within the material are limited [6], this will apply strain to the C_{60} film resulting in the disordered interface layer seen in Fig. 3a.

We note that our results support those in Refs. [8] and [12]. As C_{60} grows on top of Bi_2Se_3 by vdW epitaxy, only tunnelling events will result in charge transfer between the bulk of the topological insulator and the organic semiconductor [9, 10]. As such, there should be very little hybridisation between the C_{60} bands and the Bi_2Se_3 bulk, as seen for C_{60} in Ref. [8] and Bi_2Se_3 in Ref. [12]. We have also highlighted the need for atomically flat Bi_2Se_3 substrates in potential organic-topological insulator heterostructures, due to the existence of bismuth dangling bonds at the Bi_2Se_3 terrace step-edge.

4 Further Information

The Royce Deposition System is a multichamber, multitechnique thin film deposition tool based at the University of Leeds as part of the Henry Royce Institute. Materials from the Royce Deposition System are available as a facility service and for collaborations.

References

1. A. A. Taskin *et al.*, *Physical Review Letters* (2012).
2. C. X. Liu *et al.*, *Phys Rev Lett* **100**, 236601 (23 2008).
3. B. Yan *et al.*, *physica status solidi (RRL) - Rapid Research Letters* **7**, 148–150, ISSN: 18626254, (http://doi.wiley.com/10.1002/pssr.201206415) (1-2 Feb. 2013).
4. C. L. Song *et al.*, *Applied Physics Letters* **97**, 143118, ISSN: 00036951, (http://aip.scitation.org/doi/10.1063/1.3494595) (14 Oct. 2010).
5. N. Bansal *et al.*, *Thin Solid Films* **520**, 224–229, ISSN: 00406090 (1 Oct. 2011).
6. A. Koma, *Thin Solid Films* **216**, 72–76, ISSN: 00406090 (1 Aug. 1992).
7. R Flammini *et al.*, *Nanotechnology*, (https://doi.org/10.1088/1361-6528/aaa2c4) (2018).
8. D. W. Latzke *et al.*, *Phys. Rev. B* (2019).
9. S. Braun *et al.*, *Advanced Materials* **21**, 1450–1472, ISSN: 09359648, (http://doi.wiley.com/10.1002/adma.200802893) (14-15 Apr. 2009).
10. W. W. Pai *et al.*, *Physical Review Letters* **104**, 036103, ISSN: 00319007 (3 Jan. 2010).
11. T. Moorsom *et al.*, *Science Advances* **6**, eaax1085, ISSN: 23752548 (12 Mar. 2020).
12. S. Jakobs *et al.*, *Nano Letters* **15**, 6022–6029, ISSN: 15306992 (9 Sept. 2015).
13. A. Dodabalapur *et al.*, *Science* **269**, 1560–1562, ISSN: 00368075 (5230 Sept. 1995).
14. K. S. S. *et al.*, *Journal of Physics-Condensed Matter*, (https://doi.org/10.1088/1361-648X/ab6741) (2020).
15. M. Cinchetti *et al.*, *NATURE MATERIALS* | **16**, 25, (www.nature.com/naturematerials) (2017).
16. A. Manivannan *et al.*, "Van der Waals Epitaxial Growth of C 60 Film on a Cleaved Face of MoS 2", p. 1892.
17. S. Nakajima, *Journal of Physics and Chemistry of Solids* **24**, 479–485, ISSN: 00223697 (3 Mar. 1963).
18. D. L. Dorset *et al.*, *Acta Crystallographica Section A* **50**, 344–351, ISSN: 16005724 (3 May 1994).
19. M. V. W. Barcote *et al.*, *Materials Chemistry and Physics* **223**, 109–113, ISSN: 02540584 (Feb. 2019).
20. T. Moorsom *et al.*, *Appl. Phys. Lett* **105**, 22408, (http://dx.doi.org/10.1063/1.4885336]) (2014).
21. D. Jing *et al.*, *European Journal of Mechanics / A Solids* **28**, 948–954, (http://me.tsinghua.edu.cn/zengp/dme310/eng/eng_index.htm) (2009).
22. A. Goel *et al.*, (www.elsevier.com/locate/carbon) (2004).
23. X. H. Zhang *et al.*, *Phys Rev Lett* **103**, 106602 (10 2009).
24. L. A. Walsh *et al.*, *ACS Nano* **12**, 6310–6318, ISSN: 1936086X (6 June 2018).
25. M. Brahlek *et al.*, *Applied Physics Letters* **99**, 012109, ISSN: 00036951, (http://aip.scitation.org/doi/10.1063/1.3607484) (1 July 2011).